WESTERN OCEANUS PROCELLARUM AS SEEN BY C1XS ON CHANDRAYAAN-1. S. Z. Weider[1,2], B. J. Kellett[2], B. M. Swinyard[2,3], I. A. Crawford[1], K. H. Joy[1,2,4] and the C1XS team. [1]Centre for Planetary Sciences, Birkbeck/UCL Research School of Earth Sciences, Gower Street, London, WC1E 6BT, UK (s.weider@ucl.ac.uk), [2]Space Science & Technology Department, Rutherford Appleton Laboratory, Didcot, Oxon, OX11 0QX, UK, [3]Department of Physics & Astronomy, UCL, Gower Street, London, WC1E 6BT, UK, [4]Center for Lunar Science & Exploration, The Lunar & Planetary Institute, USRA, 3600 Bay Area Blvd, Houston, TX 77058,

Introduction: C1XS (Chandrayaan-1 X-ray Spectrometer) was a compact XRF (X-ray fluorescence) spectrometer that flew onboard the Indian Space Research Organisation's Chandrayaan-1 lunar mission between October 2008 and August 2009. Its design exploited heritage from the D-CIXS instrument on SMART-1 [1, 2], but C1XS was a more scientifically capable instrument [3-5]. The aim of the experiment was to measure the abundances of major rock-forming elements (e.g. Mg, Al, Si, Ca, Ti and Fe) in the lunar regolith at both high spectral (~110 eV) and spatial (~50 km footprint) resolutions during solar X-ray flare events reaching C-class (10^{-6} to 10^{-5} Wm^{-2}) levels or above.

Planetary XRF. This process requires solar X-rays (emitted during flare events) with sufficient energy to ionise atoms in the top few hundred microns of planetary regoliths. Electrons contained in the outer shells of the ionised atoms fall down and fill the lower energy shell vacancies created during ionisation, causing a release of energy in the form of an X-ray photon whose energy is characteristic to the element from which it originated. X-ray spectrometers such as C1XS measure the X-ray flux from a planet in terms of energy in order to estimate the concentration of major rock-forming elements in the surface. Planetary XRF is limited to bodies in the inner solar system (where the solar X-ray flux is sufficient) and to those without atmospheres (that would otherwise absorb the incident X-rays), such as the Moon, Mercury and asteroids [6].

Oceanus Procellarum flare: On 10th Februrary 2009 between 23:07:54 U.T. and 23:25:09 U.T. C1XS collected lunar XRF data during a B-class solar flare (10^{-7} to 10^{-6} Wm^{-2}). This observation has a ~1800 km long ground track (with a full-width footprint of 50 km) through western Oceanus Procellarum at a longitude of ~290° (Fig. 1). The analysis of this groundtrack's data provides an opportunity to meet one of the major C1XS science objectives: to study the composition and evolution of mare basalts over a number of lava flows [4]. Oceanus Procellarum consists of lava flows with variable compositions and eruption ages [e.g. 7-9]. However, the C1XS flare ground track only samples a subset of these deposits (Fig. 1). The sampled lava flows consist mostly of low-Ti (~3 wt. % TiO_2) basalts that are thought to be of Upper Imbrian age (~3.5 Ga) [9]. The ground track is more variable in terms of FeO content than TiO_2 (according to maps generated from Clementine multispectral data), and as such the diversity of the whole of Oceanus Procellarum is much better represented by the range of FeO contents, than by the relatively constant TiO_2 abundances.

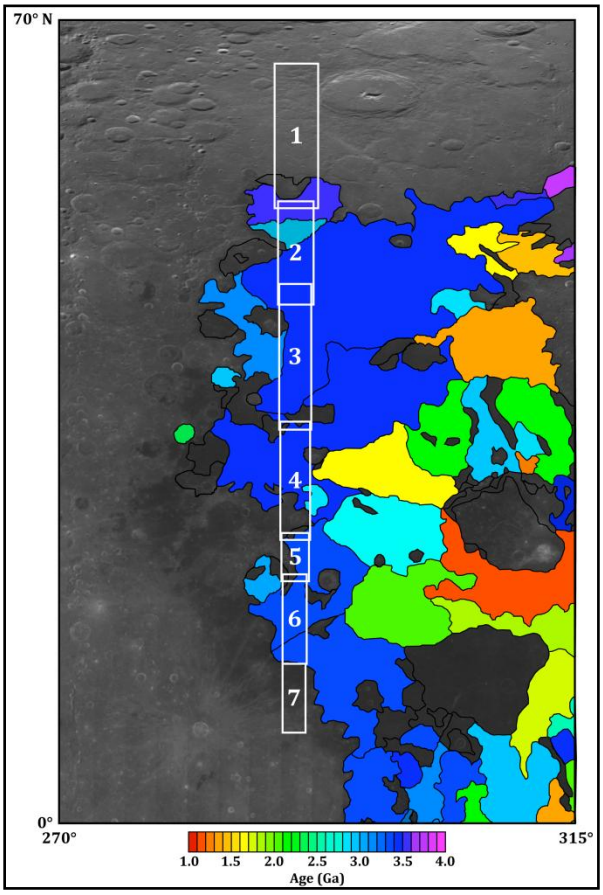

Figure 1: Clementine albedo image of Oceanus Procellarum with superimposed geological lava flow units mapped by [9]. Also shown is the groundtrack of the C1XS observation on 10th February 2009 that has been sub-divided into seven regions of interest (ROI).

Spectral modelling: The scientific analysis of all planetary XRF datasets requires an algorithm that converts X-ray fluxes to elemental abundances and ratios in order to make geological interprations about the target body. The X-ray background subtracted data (e.g. Fig. 2) presented here are modeled using the *RAL abundance algorithm* [10] which follows the fundamental parameters approach [11, 12].

The algorithm requires an incident solar X-ray spectrum for the flare period as an input and this must

contain both the bremsstrahlung and characteristic elemental lines. Although an X-ray solar monitor (XSM: [13]) accompanied C1XS onboard Chandrayaan-1 for this purpose, the B-class flare analysed here was below its detection capabilities [13]. The *atomdb* (version 2.0.0) database and modelling software (Harvard Chandra X-ray Center: http://cxc.harvard.edu/atomdb/features_idl.html) has instead been used to generate solar X-ray spectra at two temperatures (3.1 MK and 4.0 MK) likely for this flare.

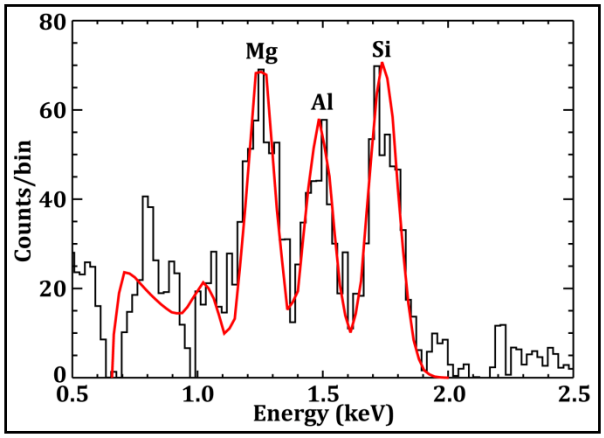

Figure 2: Background subtracted, C1XS spectrum (0.5 - 2.5 keV) for ROI 3 of the observation (see Fig. 1). The characteristic Mg, Al and Si K_α lines are well resolved (no higher energy lines are excited during this low-magnitude flare). The modelled fit (red line) is generated using a solar flare model at a temperature of 3.1 MK. The lines below ~1.0 keV are due to scattered solar X-rays rather than XRF.

Results: The algorithm fitting results for the seven flare ROI (Table 1 and Fig. 3), are expressed as the mean MgO/SiO_2 and Al_2O_3/SiO_2 ratios from modelling the flare at both 3.1 MK and 4.0 MK. The errors presented combine the 1 σ fitting errors and the range in values provided by the two temperatures. The Lunar Prospector γ-ray data for the flare region, as well as lunar sample compositions are shown for comparison.

Discussion: The C1XS results presented generally confirm the geochemical similarity of the different lava flows that have been observed in this part of Oceanus Procellarum [e.g. 9]. The compositions can be mostly replicated with simple models that linearly mix typical feldspathic highlands (FAN) and mare basalt materials. However, for at least one, dominantly highlands region (O.P. 1: see Fig. 1), the Al_2O_3/SiO_2 ratio is lower than can be invoked with these models. The poor agreement between the C1XS results and the Lunar Propsector γ-ray compositions (more so in terms of MgO/SiO_2 than Al_2O_3/SiO_2) could be explained through some combination of: inaccuracies in our results, the γ-ray results for the low-atomic mass major elements [14], and the difference in sampling depths for the two techniques. A discrepancy between γ-ray and XRF results has been noted before from NEAR results [15] and this issue warrants further investigation.

References: [1] Grande M. et al. (2003) *PSS, 51*, 427-433. [2] Grande M. et al. (2007) *PSS, 55*, 494-502. [3] Grande M. et al. (2009) *PSS, 57*, 717-724. [4] Crawford I. A. et al. (2009) *PSS, 57*, 727-734. [5] Howe C. J. et al. (2009) *PSS, 57*, 735-743. [6] Yin L. I (1993) *Remote geochemical analysis, CUP*, pp. 199-212. [7] Pieters C. M. (1978) *LPS IX*, 2825-2849. [8] Wilhelms D. E. et al. (1987) *The Geologic history of the Moon, USGS*. [9] Hiesinger H. et al. (2003) *JGR, 108* (E7), 5065. [10] Swinyard B. et al. (2010) *ESA SP-687*. [11] He F. & Van Espen P. J. (1991) *Anal. Chem., 63*, 2237-2244. [12] Clark P. E. & Trombka J. I. (1997) *JGR, 102*, 16,361-16,384. [13] Huovelin J. et al. (2002) *PSS, 50*, 1345-1353. [14] Wöhler C. et al. (2011) *PSS, 59*, 92-110. [15] Lim L. F. & Nittler L. R. (2009) *Icarus, 200*, 129-146. [16] Prettyman T. H. et al. (2006) *JGR, 111*, E12007. [17] McKay D. S. et al. (1991) *Lunar Sourcebook, CUP*, pp. 285-356. [18] Papike J.J. et al. (1998) *Rev. Min., 36*, 5.1-5.234.

Table 1: Mean MgO/SiO_2 and Al_2O_3/SiO_2 ratios for the flare's ROI (see results section for details). These C1XS values are compared with the mean Lunar Prospector (L.P.) γ-ray results [16] for the pixels which coincide with the C1XS regions. The two datasets generally agree in terms of Al_2O_3/SiO_2, but the C1XS numbers are systematically lower in terms of MgO/SiO_2.

	MgO/SiO_2		Al_2O_3/SiO_2	
ROI	**C1XS**	**L.P.**	**C1XS**	**L.P.**
O.P. 1	0.09 ± 0.03	0.21	0.31 ± 0.07	0.56
O.P. 2	0.07 ± 0.03	0.23	0.31 ± 0.06	0.42
O.P. 3	0.18 ± 0.05	0.27	0.31 ± 0.07	0.40
O.P. 4	0.14 ± 0.03	0.25	0.30 ± 0.05	0.34
O.P. 5	0.19 ± 0.05	0.22	0.39 ± 0.08	0.30
O.P. 6	0.13 ± 0.03	0.24	0.32 ± 0.06	0.32
O.P. 7	0.14 ± 0.04	0.24	0.38 ± 0.07	0.44

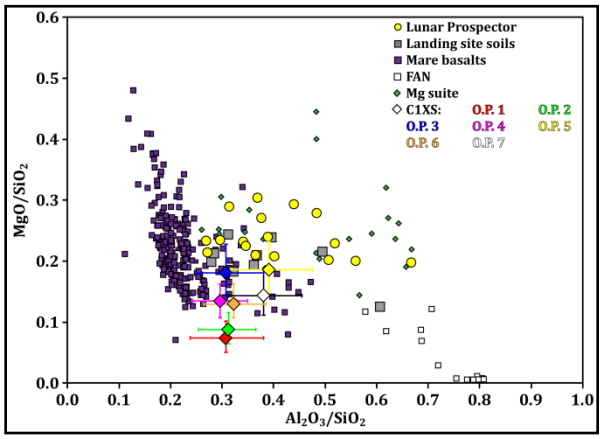

Figure 3: MgO/SiO_2 vs. Al_2O_3/SiO_2 plot showing the abundance ratio derived for each flare ROI (as given in Table 1). Also shown are: the Lunar Prospector γ-ray data [16] for pixels whose coordinates overlap with the flare groundtrack; the average landing site soil compositions [17]; and sample compositions for various lunar lithologies [18].